

**Metal organic framework based mixed matrix membranes: an increasingly important field of research with a large application potential.**

Beatriz Zornoza<sup>a</sup>, Carlos Tellez<sup>a</sup>, Joaquin Coronas<sup>a</sup>,

Jorge Gascon<sup>b\*</sup> and Freek Kapteijn<sup>b</sup>

j.gascon@tudelft.nl

<sup>a</sup> Chemical and Environmental Engineering Department and Instituto de Nanociencia de Aragón (INA), Universidad de Zaragoza, 50018 Zaragoza, Spain

<sup>b</sup> Catalysis Engineering – Chemical Engineering Dept, Delft University of Technology, Julianalaan 136, 2628 BL Delft, The Netherlands

**Abstract:** The combination of metal organic frameworks (MOFs) and polymers in the form of mixed matrix membranes (MMMs) has become an increasingly important field of research over the last few years. The first examples of membranes outperforming state of the art polymers have already been presented, emphasizing the high application potential of these composites. In this paper, the recent progress on the topic is thoroughly reviewed and the main advantages and limitations of the use of MOFs as MMMs fillers are evaluated.

**Keywords:** separation, metal organic framework, membrane, mixed matrix membrane, pervaporation.

## 1. Introduction

As energy costs rise, membrane technology is likely to play an increasingly important role in reducing the environmental impact and operational costs of industrial processes. Furthermore, gas separation membrane units are smaller than other types of plants, like amine stripping, and therefore have relatively small footprints.[1] With this decreasing in the ratio between equipment size and production capacity, membrane technologies address the requirements of process intensification.[2] Conventional technologies, such as distillation and absorption based processes, require a phase change in the mixture that is to be separated. This phase change adds a significant energy penalty. Membrane gas separation, on the other hand, does not require a phase change.[3]

Separation through membranes is usually based on the size and shape of the molecules to be separated and on their interaction with the membrane material.[4] Despite the superior performance of membranes only based on crystalline materials with well defined pore systems like zeolites [4, 5] or metal organic frameworks (MOFs),[6] low flux polymeric membranes rule the commercial scene thanks to their easy processing and mechanical strength.[7] Furthermore, synthetic reproducibility and therefore scale up of pure zeolite- or MOF-based membranes is still a major bottleneck, [8] as recently discussed by Caro.[9]

However, the existing polymeric membrane materials are not optimal: improvement in permeability is always at the expense of selectivity, and vice versa (see Figure 1).[10] Meantime, plasticization hampers the application of polymeric membranes at high pressures since high concentration of adsorbates might swell and

dilate the polymer, increasing the mobility of the polymer chains. The overall result is a reduction in the membrane selectivity far below the pure-gas values. [7]

During the last few decades, several solutions have been proposed to boost the performance of polymeric membranes. Various polymers have been modified with inorganic fillers such as zeolites, mesoporous silicas, activated carbons, carbon nanotubes and even non-porous solids to produce mixed matrix membranes (MMMs).[11-15] A MMM is an intimate and homogeneous dispersion of filler particles in a polymeric matrix. Both polymer and filler properties affect MMM morphology and separation performance.[16, 17] Regarding the filler, its chemical structure, surface chemistry, particle size distribution and aspect ratio are the most important variables. Indeed, poor filler-polymer compatibilities and filler segregation or blocking of its porosity by the polymer are the main reasons why traditional MMM fillers like zeolites, silicas or activated carbons have not made the final steps towards industrial implementation. Due to these limitations, in general only low filler loadings can be achieved without compromising the separation performance unless laborious filler post-treatments are applied. [18, 19] As to the polymer, mostly low flux glassy polymers result in MMMs with enhanced separation performance, while MMMs of highly permeable, poorly selective rubbery polymers have hardly been successful when using inorganic fillers.[16, 17]

Recent advances have shifted towards the addition of new fillers, namely carbon nanotubes, layered silicates (sometimes after delamination) and MOFs as potential fillers in the polymer matrix. [20] MOFs are among the most sophisticated nanostructured materials. Next to a high surface area and pore volume, their chemical environment can be fine-tuned by selecting the appropriate building blocks

[21] and/or by post-synthetic modification.[22] More importantly, the porosity of MOFs is, in general, much higher than that of their inorganic counterpart, zeolites, justifying the designation ‘framework’ and challenging the scientific community to make an effective use of such an empty space. In addition to the facile functionalization, many MOFs are known to undergo structural changes upon adsorption of different molecules (‘breathing’),[23, 24] facilitating the design of, for instance, dynamic composites.

Given the vast possibilities that MOFs offer in terms of design together with their intrinsic hybrid nature, it was only a matter of time until the first MOF based MMMs were reported. The incorporation of MOFs into a polymer matrix for gas separation was first explored by Yehia et al. [25] Since then, this field of research has experienced a rapid growth and the first examples of outstanding MMMs have been reported in the literature. With this manuscript, we critically review the progress made on MOF-based MMMs since the seminal work of Yehia et al. with the aim of exploring the main limitations and opportunities that MOFs offer as MMM fillers.

## **2. Preparation, testing and modelling of MOF mixed matrix membranes**

### **a) Preparation and testing**

In principle, the lab-scale fabrication procedure of MOF-based MMMs is similar to the one applied for the synthesis of other MMMs. In the general procedure for the preparation of MMMs the first step is the dispersion of the filler in the solvent in an ultrasonic bath. Polymer is then added, usually maintaining a ratio 90/10 wt. % solvent/filler-polymer mixture. The whole mixture is stirred overnight. Before the casting, different intervals of sonication and stirring take place to ensure a well

dispersion. Subsequently, the membranes are cast on a flat surface, either Petri-type dishes or Doctor Blade system, and then left overnight for evaporation of solvent at room temperature. Once dried, the films are placed in a vacuum oven for 24 h at a specific temperature (depending on the polymer glass transition temperature) high enough to remove the remaining solvent. Figure 2 presents the general procedure for the MMM preparation.

Permeability and separation factor are the two key parameters generally used to characterize polymeric membranes. Permeability  $P_A$ , a normalized productivity of a specific gas component by the membrane, is defined (Eq. 1)[26] as the gas diffusive *Flux* of the gas  $A$  through the membrane (flow per unit area  $A$ ) normalized by the partial pressure difference of that component across the membrane per unit thickness of the membrane,  $\frac{\Delta p_A}{\ell}$ .

$$(Eq. 1) \quad \begin{aligned} P_A &= \frac{Flux_A \cdot \ell}{\Delta p_A} \\ Flux_A &= \frac{Flow_A}{A} \end{aligned}$$

Permeability values are typically reported in Barrer units ( $1 \text{ Barrer} = 1 \cdot 10^{-10} \text{ cm}^3(\text{STP}) \cdot \text{cm} \cdot \text{cm}^{-2} \cdot \text{s}^{-1} \cdot \text{cmHg}^{-1} = 3.348 \cdot 10^{-16} \text{ mol} \cdot \text{m} \cdot \text{m}^{-2} \cdot \text{Pa}^{-1} \cdot \text{s}^{-1}$ ).

The separation factor reflects the capability of a polymer membrane to separate one gas from another. If the permeabilities of two individual components are known, the ideal selectivity,  $S_{AB}$  (Eq. 2), is given by the ratio of the two pure gas permeabilities:

$$S_{AB} = \frac{P_A}{P_B} \quad (\text{Eq. 2})$$

For permeation of actual A/B mixtures, the mixed gas selectivity, also called separation factor ( $\alpha_{AB}$ ), is calculated from composition analysis as the ratio of the mole fractions of the components in the permeate stream,  $y$ , and the feed stream,  $x$  (Eq. 3). In the case where the gases do not interact strongly with each other or with the membrane material, the ideal selectivity is equal to the actual separation factor, but frequently this is not the case.

$$\alpha_{AB} = \frac{(y_A / y_B)}{(x_A / x_B)} \quad (\text{Eq. 3})$$

For every MOF-polymer couple, the MOF loading should be maximized. Figure 3 illustrates the usual effect of MMM MOF filler loading over selectivity and permeability. Loadings lower than a certain value do not alter in a significant way the transport properties of the polymer membrane, while rigidity and mechanical strength of the composite are increased, as determined by differential scanning calorimetry and dynamic mechanical analysis.[14, 27-30] At a certain loading, a good dispersion of the filler with an excellent interfacial contact with the polymer chains (composite interface) results in an optimum MMM performance. However, at higher loadings polymer chains are not completely able to intimately surround the particles that may agglomerate reducing dispersion within the polymer matrix and forming undesirable channels.[31, 32] High permeabilities are also attributed to the

disruption of the polymer chain packing and linking due to the presence of the molecular sieves which implies also an increase in polymer free volume.[33]

b) Engineering models to describe permeation through MMMs

In spite of the considerable interest devoted to MMMs during the last few decades, models for predicting performance of these composites have been scarcely proposed. Barrer and Petropoulos were the first proposing a model for the performance of polymer-filler blends.[34] Their formulation assumes concentration-independent diffusivities and Henry's law adsorption, and it deals with the inherent two-dimensionality of the situation through the introduction of several unknown correction factors. The reliance on such correction factors is one good reason to seek more satisfying treatments; the restrictive assumption of Henry's law adsorption is another. Cussler has proposed perhaps the most sophisticated model by reducing the three-dimensional diffusion problem to an essentially one-dimensional problem through a series of approximations.[35] Aside from the limitations of these approximations, Cussler's model employs Fickian diffusivity with a constant diffusivity and an equilibrium condition between phases that requires identical adsorption isotherms in both materials. These are both serious limitations, particularly when trying to describe the performance of a composite containing a zeolite phase. The Maxwell-Stefan formulation can be also extended to MMMs by combining flux through the polymer and filler in parallel and series pathways, in a clear analogy to electrical circuits. This model is however only applicable for low filler loadings since it assumes that the streamlines associated with diffusive mass transport around filler particles are not affected by the presence of nearby particles.

The Bruggeman model,[36] which can be considered to be an improved version of the Maxwell model, accounts for these effects and extends the applicability of Maxwell-Stefan diffusivities to highly loaded MMMs.[37] Sheffel and Tsapatsis [38, 39] introduced later a more extended model for diffusive transport in microporous MMMs utilizing the Maxwell–Stefan formulation and different models to account for multi-component mixtures: Henry’s law, extended Langmuir model, and ideal adsorbed solution theory (IAST).

Any model attempting to describe diffusion within a membrane containing a microporous filler phase must include a realistic treatment of diffusion in both the porous filler and the continuous phase.

Diffusion in the gas phase or in relative large pores (>100 nm [40]) is dominated by inter-molecular collisions and the flux of component  $i$  can be described by the Maxwell-Stefan (MS) approach, [41] in which forces acting on molecules (in diffusional processes the gradient in thermodynamic potential) are balanced by the friction between molecules and, in case of porous materials, with a solid. In the latter case this model was named the ‘Dusty Gas Model’. The often used Fick’s law is a simplification of the generalized MS equations for thermodynamically ideal systems. [41]

While Fickian diffusion can be used to describe transport through polymers, in the case of a porous material a correction needs to be made to account for the porosity ( $\varepsilon$ ) and tortuosity ( $\tau$ ) of the material, leading to an ‘effective’ diffusivity. In this way, molar flux ( $N_i$ , mol m<sup>-2</sup> s<sup>-1</sup>) can be defined as:

$$N_i = -\frac{\varepsilon}{\tau} D_i \nabla C_i = -D_i^{eff} \nabla C_i \quad (\text{Eq. 4})$$

In porous materials, when the mean free path of a molecule is in the order of or larger than the pore diameter ( $\sim 10\text{-}100\text{ nm}$ ) molecule-wall collisions start to dominate and the diffusivity can be described by the Knudsen diffusion mechanism. A flux in such small pores can be presented as:

$$N_i = -\frac{\varepsilon}{\tau} D_{Kn,i} \nabla C_i, \quad D_{Kn,i} = \frac{d_0}{3} \sqrt{\left( \frac{8RT}{\pi M_i} \right)} \quad (\text{Eq. 5})$$

In the case of zeolites and MOFs, the pores approach molecular dimensions ( $\sim 0.3\text{-}0.74\text{ nm}$ ) and, consequently, mass transport through such pores is determined by the interaction of the molecules with the pore wall. Now molecules are adsorbed, have lost their gaseous nature, and transport is often referred to as surface or zeolitic diffusion.[40] The flux can now also be represented in a Fickian way; the concentration ( $q_i$ ) represents the adsorbed amount or loading. A common unit for the loading is  $\text{mol kg}^{-1}$ , therefore the adsorbent density ( $\rho$ ) is added to arrive at consistent dimensions. Note that the diffusivity in this case has a different magnitude by this definition (compare Eq.6 and 5), about a factor of the Henry constant for adsorption.

$$N_i = -\rho D_i \nabla q_i \quad (\text{Eq.6})$$

The tortuosity and porosity presented in equation (4) are not specified in equation (6), these are an inherent property of the diffusivity. Each adsorbent has its own specific pore network with its own tortuosity and porosity. Moreover, the pore network can be 1-, 2- or 3-dimensional with different pore sizes or connectivities in different directions leading to diffusion anisotropy.[42]

The adsorbed phase ( $q_i$ ) in equation (6) is related to the gas phase fugacity through an adsorption isotherm of which the classical example is the Langmuir isotherm:

$$q_i = \frac{q_i^{sat} K_i p_i}{1 + K_i p_i} \quad (\text{Eq. 7})$$

An important difference between gas phase and adsorbed phase diffusion is the concentration level, being much higher in the case of adsorbed phase diffusion. When the gradient in chemical potential is taken as the fundamental driving force for diffusion [40, 41] a correction needs to be made to equation (6). Now, a so-called thermodynamic correction factor ( $\Gamma_{ii}$ ) is introduced; the diffusivity is referred to as ‘corrected’ or ‘Maxwell Stefan’ (MS) diffusivity.

$$N_i = -\rho \mathbf{D}_i \nabla \ln f_i = -\rho \mathbf{D}_i \Gamma_{ii} \nabla q_i, \quad \Gamma_{ii} = \frac{d \ln f_i}{d \ln q_i} \quad (\text{Eq. 8})$$

For a single site Langmuir isotherm the thermodynamic correction factor is given by:

$$\Gamma_{ii} = \frac{d \ln f_i}{d \ln q_i} = \frac{1}{1 - \theta_i}, \quad \theta_i = \frac{q_i}{q_i^{sat}} \quad (\text{Eq. 9})$$

In the limit of low loading the thermodynamic correction factor approaches 1 and the MS and Fickian diffusivity are equal. Although the MS diffusivity appears to be physically more correct, the Fickian diffusivity remains very important since this diffusivity can be directly assessed in diffusion measurements.

When multicomponent adsorption needs to be considered (i.e. separation through membranes), due to the relatively high concentrations of adsorbates, interactions between molecules can play a significant role in terms of ‘speeding up’ or ‘slowing down’ other components. In the Maxwell-Stefan approach besides the interaction (or ‘friction’) of the individual molecule with pore walls, also the interaction between the different diffusing molecules is accounted for and balanced with the driving force for mass transport:

$$\rho\theta_i \nabla \ln f_i = \sum_{j=1}^n \frac{q_j N_i - q_i N_j}{q_j^{sat} q_i^{sat} \mathcal{D}_{ij}} + \frac{N_i}{q_i^{sat} \mathcal{D}_i}; \quad i = 1, 2 \dots n \quad (\text{Eq. 10})$$

Within this approach the estimation of  $\mathcal{D}_{ij}$  can be difficult, however, a reasonable estimation can be made through a logarithmic ('Vignes') interpolation [41, 43, 44] based on the single component exchange diffusivities and a correction factor  $F$  for the confinement of the molecules in the narrow zeolite pores.[45]

For a single component system of tagged and untagged species the saturation capacities are equal and one can show [45] that the single component exchange coefficient is related to the self diffusivity and MS diffusivity as

$$\frac{1}{D_{Self,i}} = \frac{1}{\mathcal{D}_i} + \frac{1}{\mathcal{D}_{ii}}, \quad (\text{Eq. 11})$$

$$\mathcal{D}_{ij} = F \cdot \mathcal{D}_{ii}^{\frac{\theta_i}{\theta_i + \theta_j}} \mathcal{D}_{jj}^{\frac{\theta_j}{\theta_i + \theta_j}} \quad (\text{Eq. 12})$$

For mesoporous systems the factor  $F$  equals 1, while for the microporous materials values  $<1$  hold. [45]

It is evident that in the case of mixture diffusion an accurate estimation of the individual component loading and the driving force is required to satisfactory model such a system. For zeolitic and MOF systems, the Ideal Adsorbed Solution Theory (IAST) [46] provides an acceptable mixture prediction based on the single component isotherms [40, 47, 48], but when adsorption heterogeneity becomes manifest IAST also tends to fail.[49]

At significant loading the molecular interaction can play an important role, strongly influencing the reactant and product concentration profiles. When the

loading is relatively low the cross-correlation effects can often be ignored, i.e. the system can be modelled as single component system (Eq. (8)).

Once diffusion and adsorption for both components have been defined, a model able to describe transport through the composite can be established. For instance, the Maxwell model can be used to describe the effective molar flux ( $N_{eff}$ ) of a gas species in a MMM for a suspension of spherical filler particles in a continuous polymer matrix as: [37, 50, 51]

$$N_{eff} = N_c \left[ \frac{N_d + 2N_c - 2\phi_d(N_c - N_d)}{N_d + 2N_c + \phi_d(N_c - N_d)} \right] \quad (\text{Eq. 13})$$

In this expression,  $N_c$  and  $N_d$  represent the molar fluxes in the continuous and dispersed phases, respectively, and  $\phi_d$  is the volume fraction of the dispersed phase. The Maxwell model combines flux through the polymer and filler in parallel and series pathways, similar to electrical circuits. The Maxwell model is intended to be applicable for low filler loadings since it assumes that the streamlines associated with diffusive mass transport around filler particles are not affected by the presence of nearby particles. The Bruggeman model,[36, 37] which can be considered to be an improved version of the Maxwell model, accounts for these effects and defines for spherical particles the effective flux in an implicit relation:

$$\left[ \frac{\left( \frac{N_{eff}}{N_c} \right) - \left( \frac{N_d}{N_c} \right)}{1 - \left( \frac{N_d}{N_c} \right)} \right] \left( \frac{N_{eff}}{N_c} \right)^{1/3} = (1 - \phi_d) \quad (\text{Eq. 14})$$

The Maxwell and Bruggeman models give similar results up to  $\phi_d=0.2$ . [36] Both models describe the permeation of a pure gas through a membrane. Once the

effective permeabilities of two gas species are calculated, the ideal selectivity,  $\alpha_{ideal(i/j)}$ , the ratio of pure gas permeabilities of each species, can be determined.

Modeling mixture permeation through MMMs is more complicated than describing pure gas permeation since the gas permeabilities of each species can be affected by competition effects between the two species. The most widely applied method for calculating mixture permeation is the so-called dual mode/partial immobilization model. [37, 52] The model proposes that sorption can occur in either the Langmuir or the Henry's Law regime (i.e. dual mode sorption) and that the diffusion through these regimes can also be different (partial immobilization). This approach is only based on parameters supplied by pure gas measurements. In this case, the generalized expressions for the permeability coefficients of species A and B in a binary gas mixture with a vacuum downstream are:

$$P_A = K_A^H D_A^H \left( 1 + \frac{F_A K_A}{1 + b_A f_A + b_B f_B} \right) \quad (\text{Eq. 15})$$

$$P_B = K_B^H D_B^H \left( 1 + \frac{F_B K_B}{1 + b_A f_A + b_B f_B} \right) \quad (\text{Eq. 16})$$

where and  $F_A = \frac{D_A^L}{D_A^H}$ ,  $F_B = \frac{D_B^L}{D_B^H}$ ,  $K_A = \frac{C_A^{sat} b_A}{K_A^H}$ ,  $K_B = \frac{C_B^{sat} b_B}{K_B^H}$ , and  $f_A$  and  $f_B$  correspond

to the upstream fugacities of components A and B. In these expressions,  $D_i^H$  and  $D_i^L$  are the diffusivities of species  $i$  in the Henry and Langmuir environments, respectively;  $K_i^H$  is the Henry adsorption coefficient of species  $i$ , and  $C_i^{sat}$  and  $b_i$  are the Langmuir capacity constant and affinity constant for species  $i$ , respectively.

When it comes to MOF-MMMs, performance modeling has hardly been explored. Keskin and Sholl [50] studied MMMs consisting of Matrimid<sup>®</sup> and MOF-5 by using Maxwell and Bruggeman permeation models to predict single gas permeabilities for low and high filler loadings respectively. To calculate mixture permeation, the authors applied a dual mode/partial immobilization method, results are discussed later in the text.

### 3. MOF MMMs

Gas permeation transport in MMMs is governed mainly by a solution-diffusion mechanism due to their higher fraction of continuous polymer matrix. However, through the dispersed fillers, the MOF in our case, two permselective gas transport mechanisms are favoured: (i) adsorbate-surface interactions, concerning chemical and/or physical interaction between the adsorbent and the adsorbate; and (ii) size-exclusion, related to the dimension and shape of the framework pores and molecules [53].

The use of MOFs in MMMs offers potential advantages over other nanostructured porous materials mostly due to: (i) control of the MOF-polymer interface interaction is easier, since organic linkers of MOFs have a better affinity for the polymer chains than other inorganic fillers. This compatibility helps avoiding the so-called “sieve-in-a-cage morphology”, a gap between the phases [54-56], the most common MMM deficiency and (ii) the size, shape and chemical functionalities of their cavities can be easily adjusted by choosing the appropriate ligands in the

synthesis [21] or by post-synthetic functionalization [22]. When comparing MOFs with other fillers, it needs to be considered that MOFs commonly have a higher pore volume and a lower density than zeolites, meaning that their effect on the membrane properties can be larger for a given weight percentage of the filler [57]. Related to the interfacial compatibility, filler particle size and shape play an important role. For instance, according to a previous work, the use of mesoporous silica [14, 58] or hollow silicalite-1 [15] spherical particles of a few micrometer in size with a narrow size distribution facilitated the production of highly homogeneous MMMs, minimizing agglomeration and therefore improving dispersion and interaction with the polymer mostly due two main reasons: (i) the spherical shape helps the contact between the particles within the polymer and (ii) the micron particle size avoids agglomeration of particles. [14]

The first MOF-MMM [25] comprised a three dimensional copper(II) biphenyl biphenyl dicarboxylate-triethylenediamine MOF embedded in PAET (poly(3-acetoxyethylthiophene)) for gas separation. The resulting composite displayed an enhanced CH<sub>4</sub> permeability at 20 and 30 wt. % of MOF loading. The authors claimed that the increase in hydrophobicity of the MMMs might preferentially increase the adsorption of methane in the copper MOF, resulting in an increase in permeability. However, a decrease in CO<sub>2</sub> permeability, and therefore a reduction of the CO<sub>2</sub>/CH<sub>4</sub> was observed. Since this pioneering work, the interest in MOF-MMMs has been growing and it has already been demonstrated that, by choosing the proper MOF-polymer couple, it is possible to surpass the Robeson's upper bound [59] for several important separations, approaching the commercially attractive region.

To date, only the use of a few different polymers and MOFs in the form of MMMs has been reported. These works can be separated into those using *low flux polymers* (PSF: polysulfone [31, 60-64]; PPEES: poly(1,4-phenylene ether-ether-sulfone) [65]; PVAc: polyvinyl acetate [66]; polyetherimide Ultem® [57]; polyimide Matrimid® [29, 32, 57, 67-71]; PBI (polybenzimidazole); and those dealing with *high flux polymers* (PDMS: polydimethylsiloxane [31, 68], PMPS: polymethylphenylsiloxane [72] and 6FDA-DAM: 2,2-bis(3,4-carboxyphenyl) hexafluoropropane dianhydride-diaminomesitylene). [57, 73] In the classification below, glassy polymers are considered low flux polymers ( $P_A < 50$  Barrer), while rubbery polymers usually give rise to higher fluxes ( $P_A > 100$  Barrer).

In Table 1, a chronological summary of the different MOF-MMMs published in the literature is presented. The major application of the resulting MMMs is gas separation (GS) but also pervaporation (PV) and solvent resistant nanofiltration (SRNF) have already been reported.

It has to be considered that comparison of MMMs is not straightforward. In Table 1, for the GS membranes, the performance in the separation of CO<sub>2</sub> from CH<sub>4</sub> is used as “standard” comparison, with the reported values represented in a Robeson-type plot in Figure 4. The optimum permselectivity results are given between brackets and correspond to the maximum loading of MOF that the continuous polymer phase exhibits in a defect-free MMM. From the studied MOF loadings in Table 1, the one that performed best is also given between brackets. When similar selectivities with increasing loading were found, we chose the loading that provided the highest permeabilities. Figure 5 shows the SEM micrographs of the best MOF-MMMs reported in the literature indicating the MOF loading used.

### ***3.1. Low flux polymers***

#### ***a) Classical MOF fillers***

Similar to the behaviour observed by Yehia et al. [25] for the aforementioned copper(II) biphenyl dicarboxylate-triethylenediamine MOF, Zhang et al. [29] explored the same trend with Cu-BPY-HFS (Cu-4,4'-bipyridine-hexafluorosilicate) MOF. In this case, the polyimide Matrimid<sup>®</sup> was the chosen polymer to study the pure gas permeation of H<sub>2</sub>, N<sub>2</sub>, O<sub>2</sub>, CH<sub>4</sub> and CO<sub>2</sub>, as well as the separations of CO<sub>2</sub>/CH<sub>4</sub>, H<sub>2</sub>/CO<sub>2</sub> and CH<sub>4</sub>/N<sub>2</sub> mixtures. An increase in solubility and hence of selectivity was only found towards CH<sub>4</sub> (CH<sub>4</sub>/N<sub>2</sub> separation factor from 0.95 to 1.7 with 20 wt. % of MOF) attributed to the high hydrophobicity of the MOF.

The first patent on MOF MMMs dealt with the use of IRMOF-1.[74] Up to 20 wt. % of IRMOF-1 particles were dispersed in Matrimid<sup>®</sup> polyimide and Ultem<sup>®</sup> polyetherimide. Single gas permeation measurements showed 2-3 fold improvements in CO<sub>2</sub> and H<sub>2</sub> gas permeabilities compared to the pure polymers without significant decrease in the corresponding ideal selectivities. In the same line, Perez et al. [67] reported an increase in permeability with almost constant ideal selectivity from the neat polymer (Matrimid<sup>®</sup>) to the 30 wt. % of MOF-5 for H<sub>2</sub>, CO<sub>2</sub>, O<sub>2</sub>, N<sub>2</sub> and CH<sub>4</sub>. At that loading, CO<sub>2</sub> permeability showed an increase of 55%, CH<sub>4</sub> did 100%, while the CO<sub>2</sub>/CH<sub>4</sub> separation factor increased by a 6 %. A molecular simulation study of gas mixtures permeating through MMMs containing IRMOF-1 in Matrimid<sup>®</sup> was performed by Keskin and Sholl. [50] The authors described the predicted performance of Cu(hfipbb)(H<sub>2</sub>hfipbb)<sub>0.5</sub> MMMs using Maxwell and Bruggeman models. They illustrated that 20 wt.% Cu(hfipbb)(H<sub>2</sub>hfipbb)<sub>0.5</sub> was enough to bring

the MMM above the Robeson's upper bound with a CO<sub>2</sub>/CH<sub>4</sub> selectivity of 72 and CO<sub>2</sub> permeability of 15.7 Barrer.

Cu-BDC MOF, structure synthesized from copper nitrate trihydrate and terephthalic acid (TPA), was successfully embedded in PVAc [66] obtaining improvements over the pure polymer gas transport properties for MMMs with a 15 wt. % of loading for He/CH<sub>4</sub>, O<sub>2</sub>/N<sub>2</sub>, N<sub>2</sub>/CH<sub>4</sub>, CO<sub>2</sub>/N<sub>2</sub> and CO<sub>2</sub>/CH<sub>4</sub> mixtures. A large enhancement in both permeability and selectivity for CO<sub>2</sub> suggested a potential application of these MMMs for CO<sub>2</sub> removal from natural gas.

HKUST-1 or Cu<sub>3</sub>(BTC)<sub>2</sub> (copper(II)-benzene-1,3,5-tricarboxylate) is a 3D porous MOF with a zeolite-like structure. Car et al. [31] were the first to study this MOF embedded in PSF for the transport of H<sub>2</sub>, N<sub>2</sub>, O<sub>2</sub>, CH<sub>4</sub> and CO<sub>2</sub> and compared the performance of CuBTC membranes with similar ones made using Mg(HCOO)<sub>2</sub> (magnesium(II)-formate). While HKUST-1 showed a high sorption affinity for CO<sub>2</sub> and H<sub>2</sub>, the use of Mg(HCOO)<sub>2</sub> only resulted in an increase in H<sub>2</sub> permeability. Hybrid membranes were only possible with loadings lower than a 10 wt. % of both MOFs due to the tendency of the particles to agglomerate.

Gas separation performance of Cu<sub>3</sub>(BTC)<sub>2</sub>-Matrimid<sup>®</sup> MMMs were also reported by Liu and co-workers [74]. The CO<sub>2</sub> permeability increased 121 % using a 30 wt. % loading without loss in selectivity over the bare polymer. The same trend was found for H<sub>2</sub>/CH<sub>4</sub> separation, resulting in an almost double selectivity.

Recently, polyimide Matrimid<sup>®</sup> and Matrimid<sup>®</sup>/PSF UDEL<sup>®</sup> (3:1) blends containing the same crystalline MOF, Cu<sub>3</sub>(BTC)<sub>2</sub>, were used to prepare asymmetric MMMs [68]. CO<sub>2</sub>/CH<sub>4</sub> and CO<sub>2</sub>/N<sub>2</sub> binary gas mixtures under different CO<sub>2</sub> composition as a function of filler loading were tested. In these membranes, CO<sub>2</sub> was

selectively attracted towards the unsaturated Cu atoms in the framework over CH<sub>4</sub> or N<sub>2</sub>. The same pair of materials was also used to prepare hollow fiber MMM by the dry/wet-spinning method by Hu et al. [69]. In these membranes, at 6 wt. % Cu<sub>3</sub>(BTC)<sub>2</sub> loading, the permeability of H<sub>2</sub> increased by 45 %, and the H<sub>2</sub>/CH<sub>4</sub>, H<sub>2</sub>/N<sub>2</sub>, H<sub>2</sub>/CO<sub>2</sub> and H<sub>2</sub>/O<sub>2</sub> ideal selectivities augmented by a factor of 2-3 when compared to the bare polyimide.

#### b) ZIF containing MMMs

Zeolite imidazolate frameworks (ZIFs) are a sub-family of MOFs named after the resemblance of the zeolite topologies and the metal-imidazolate-metal bond angles to the zeolite Si-O-Si angles.[75] Most ZIFs are built by connecting metal clusters (mainly Zn or Co) through functionalized imidazole linkers, resulting in the formation of small pore solids displaying zeotype architectures such as SOD, RHO or LTA, among others. The full saturation of the metal together with the use of imidazole linkers provide ZIF materials with an outstanding thermal stability (up to 400 °C) and with a highly hydrophobic character.

Diaz et al. [61] studied CO<sub>2</sub> transport in PSF membranes containing ZIF-8 (Zn(2-methylimidazole)<sub>2</sub>) using both permeation and pulse field gradient (PFG)-NMR spectroscopy at room temperature and 6 bar. As expected, gas adsorption in the MMMs rised as the filler content increased. Later, these authors reported the effect of ZIF-8 (0-30 wt. %) in poly(1,4-phenylene ether-ether-sulfone) (PPEES) MMMs. [65] The membrane with a 30 wt. % content exhibited ideal selectivities for both pair of O<sub>2</sub>/N<sub>2</sub> and H<sub>2</sub>/N<sub>2</sub> gases close to the Robeson upper bound. No significant improvements were obtained for the separation of H<sub>2</sub>/CH<sub>4</sub> and CO<sub>2</sub>/CH<sub>4</sub> mixtures.

ZIF-8/Matrimid<sup>®</sup> MMMs with loadings up to 60 wt. % were also fabricated by Ordoñez and co-workers. [32] Single permeabilities of H<sub>2</sub>, CO<sub>2</sub>, O<sub>2</sub>, N<sub>2</sub>, CH<sub>4</sub>, and C<sub>3</sub>H<sub>8</sub>, together with separation of H<sub>2</sub>/O<sub>2</sub>, H<sub>2</sub>/CO<sub>2</sub>, H<sub>2</sub>/CH<sub>4</sub>, CO<sub>2</sub>/CH<sub>4</sub>, CO<sub>2</sub>/C<sub>3</sub>H<sub>8</sub> and H<sub>2</sub>/C<sub>3</sub>H<sub>8</sub> mixtures were studied. Large improvements in the ideal selectivity at 40 wt. % loading along with a decrease at loadings higher than 50-60 wt. % due to MOF aggregation were reported.

Seoane et al. [64] studied the crystallization and activation of zeolitic imidazolate framework ZIF-20 [76] from the point of view of crystal size and aggregation by using rotation and seeding with previously prepared material. The dispersion in PSF of the small synthesized ZIF-20 particles obtained with low aggregation resulted in an improved O<sub>2</sub>-selective MMM, O<sub>2</sub> permeability and O<sub>2</sub>/N<sub>2</sub> selectivity being 1.0 Barrer and 6.7, respectively.

Finally, Yang and co-workers [30] incorporated ZIF-7 into polybenzimidazole (PBI) polymer. MMMs with ZIF-7 loadings as high as 50 wt% enhanced H<sub>2</sub> permeability without compromising the H<sub>2</sub>/CO<sub>2</sub> selectivity compared to pure PBI membranes even at elevated temperatures (up to 180 °C).

### c) MOF-zeolite MMMs

A new approach towards overperforming MMMs is the combination of fillers of different nature (MOFs and zeolites) in the same polymer matrix. Recently, mixed matrix membranes using filler mixtures containing ZIF-8 and silicalite-1 and HKUST-1 and silicalite-1, with total loadings up to 16 wt. % have been reported. [63] Certain synergy effects were found, leading to membranes with better permeation properties than those of MMMs with only one filler type. In these

membranes the different surface chemistry of both types of fillers may help dispersion inside the polymer phase. In particular, due to the high CO<sub>2</sub> adsorption of HKUST-1, the combination of HKUST-1 and silicalite-1 resulted in the best separation performance for CO<sub>2</sub>-containing mixtures. On the other hand, ZIF-8-containing MMMs gave rise to the best performance when mixtures are separated based on diffusion differences between permeating molecules.

d) Flexible MOF-containing MMMs

A special class of MOF materials are those that can reversibly change their framework when guest molecules are introduced. This behaviour results in special properties like the breathing effect [77, 78] and the gate phenomenon [79], where pores reversibly contract or open upon adsorption of molecules. An example of a breathing-type material is the MIL-53 series.

MIL-53 is built from MO<sub>4</sub>(OH)<sub>2</sub> octahedra (where M can be Fe<sup>3+</sup>, Cr<sup>3+</sup>, Al<sup>3+</sup>, Ga<sup>3+</sup>, In<sup>3+</sup> or Sc<sup>3+</sup>) and 1,4-benzenedicarboxylate (terephthalate) linkers.[78, 80] In this way a crystalline material with 1-D diamond shaped pores, with a free diameter of 8.6 Å, is formed. The MIL-53 series shows a pronounced framework flexibility: upon adsorption of guest molecules, like CO<sub>2</sub>, H<sub>2</sub>O and most organic solvents, the framework structure reversibly changes. For the Cr- or Al-forms MIL-53(Cr) or MIL-53(Al) the structure in which the pores are in the “open” form is the most stable after thermal activation. [81, 82] These two types of MIL-53 show a transition from an initial dehydrated, large pore form (*lp* form) to a narrow pore form (*np* form) during adsorption of certain molecules. When the driving force (the partial pressure of the adsorbing molecule) is large enough the pores reopen to their original large pore form.[77] The Fe- and Ga-forms MIL-53(Fe) and MIL-53(Ga) display a more

complex and different behaviour. The stability domain of the *np* structure of MIL-53(Ga) *np* is larger (up to 160 °C instead of 20–30 °C for Al, for instance) than that of MIL-53(Fe) with a very narrow pore (*vnnp*) form when it is initially dehydrated. This form can hardly accommodate guest molecules.[83-85] With increasing pressure this structure passes via intermediate forms to the *lp* form, instead of going in one time from *np* to *lp* form.

When it comes to MMMs, the use of flexible fillers might result in membranes resistant to solvents and even eliminate plasticity behaviour, provided that the flexibility of the framework is not altered during the preparation of the composite.

The first MMMs comprising a flexible filler were reported by Basu et al. [71] using high flux polymers for nanofiltration applications (discussed later). The same group reported one year later the comparison between MMMs containing HKUST-1, ZIF-8 and MIL-53(Al) [70] for the separation of CO<sub>2</sub>/CH<sub>4</sub> and CO<sub>2</sub>/N<sub>2</sub> mixtures at different CO<sub>2</sub> concentrations. Dense and asymmetric membranes, using the polyimide Matrimid® as continuous polymer phase, were obtained and resulted in enhanced separation performance with increasing filler loading (0-30 wt. %). HKUST-1 and MIL-53(Al) showed higher selectivities than ZIF-8. For HKUST-1, the increase in selectivity was attributed to the strong CO<sub>2</sub> interaction with the unsaturated metal sites. In case of MIL-53(Al) interactions with the hydroxyl groups of the framework and the breathing behaviour were claimed to enhance the CO<sub>2</sub>-MOF interaction.

Very recently, we studied the use of an amino functionalized MIL-53 (hereafter NH<sub>2</sub>-MIL-53(Al)) as filler in MMMs.[62] Microwave synthesized

homogeneous, micrometer-sized NH<sub>2</sub>-MIL-53(Al) particles were used to fabricate nanocomposite membranes with PSF Udel<sup>®</sup> P-3500. Continuous MOF-polymer matrices were obtained at loadings as high as 40 wt.%. An excellent match between polymer and MOF filler was achieved thanks to hydrogen bonding interactions between the surface amine moieties of the MOF and the sulfonic groups of the polymer (Figure 6c). Although during the preparation procedure some of the MOF particles stay in the *lp* configuration, probably because of solvent adsorption and subsequent breathing (Figure 6d), the effect of breathing on the composite, as measured using CO<sub>2</sub> adsorption up to 25 bar, was clear. In Figure 6b the contribution of the MOF to the total CO<sub>2</sub> uptake is plotted and compared with the adsorption isotherm of the pure NH<sub>2</sub>-MIL-53(Al).

At low pressures the contribution of the MOF is almost negligible, while as the CO<sub>2</sub> pressure is increased, the contribution of the MOF to the total uptake becomes more important and the rapid increase indicates even breathing of the framework, with a final total uptake similar to that of the MOF filler in its *lp* form. In comparison with the bare material, the breathing is shifted to higher pressures, while the discrete adsorption steps disappeared.

Regarding the CO<sub>2</sub>/CH<sub>4</sub> separation performance of the breathing composites, separation at RT and moderate pressures resulted in an increase in selectivity (~100%) along with a slight increase in CO<sub>2</sub> permeance (~10%). To study the effect of the MOF filler at high adsorbate loadings together with the consequences of MOF flexibility, the high-pressure performance of the different NH<sub>2</sub>-MIL-53(Al) MMMs was investigated. In order to reach high CO<sub>2</sub> loadings, experiments at reduced temperatures were performed. The combination of high pressures (10 bar) and low

temperatures (-10 °C) had beneficial effects on the separation selectivity (Figure 6a). This increase in selectivity with pressure has very important consequences for applications like natural gas and biogas upgrading, where the retentate has to be kept pressurized. In addition, this behavior is opposite to the one shown by most inorganic membranes, where decrease in selectivity at elevated pressures is an intrinsic property, [86-89] or due to the presence of small defects that become more important at high pressures.[90, 91] We speculate that the increase of selectivity is due to the intrinsic flexibility of the MOF filler: as pressure increases, adsorption in the CO<sub>2</sub> shape selective microporous MOF becomes more important (see Figure 6b). Under the conditions related to Figure 6a, the transition  $np \rightarrow lp$  happens at ca. 5 bar of CO<sub>2</sub>, when the performance of the pure polymeric membrane starts decaying. At this point, the expansion of the MOF particles might not only fill the gap between polymer chains due to the high CO<sub>2</sub> loading ('self healing' effect) but also would substantially contribute to the total flux through the membrane. As result, higher fluxes and much better selectivities were obtained resulting in membranes performing at the Robeson upper bound (see Figure 4).

### 3.2. *High flux polymers*

Rubbery polymers are flexible elastomers displaying elastic properties. They are able to resume their original shape when a deforming force is removed. When used as membrane materials, this flexibility results in very high fluxes along with low selectivities (right side of the Robeson plot in Figure 1). Although some MMMs using this type of polymers have been reported, the combination of inorganic fillers

and rubbery polymers usually does not work because of the poor polymer-filler matching.[16, 54]

The first example of the combination of a high flux rubbery polymer and metal organic frameworks as a MMM was reported by Car et al. [31] HKUST-1-polydimethylsiloxane (PDMS) composites were prepared and the performance of MMMs containing 0-40 wt. % filler was tested for H<sub>2</sub>, N<sub>2</sub>, O<sub>2</sub>, CH<sub>4</sub> and CO<sub>2</sub>. Higher fluxes were obtained for all composites. At the same time, moderate improvements in selectivity were observed at 10 and up to 10 wt. % loadings for CO<sub>2</sub>/N<sub>2</sub> and CO<sub>2</sub>/CH<sub>4</sub> mixtures, respectively.

Basu and co-workers [71] prepared PDMS MMMs containing different MOFs as fillers (ZIF-8, HKUST-1, MIL-53(Al) and MIL-47(V)). These MMMs were applied in nanofiltration, more specifically in the separation of Rose Bengal (RB) from isopropanol. In spite to the poor adhesion between the polymer and the filler, all membranes showed an enhanced solvent resistance. Strong improvements in polymer-filler matching were obtained by silylation of the MOF surfaces. Retention of the MMMs was significantly higher compared to unfilled PDMS membranes. This was explained by the effect of reduced polymer swelling and size exclusion of the filler, mostly with ZIF-8 as compared to HKUST-1, MIL-53(Al) and MIL-47(V).

As mentioned earlier, for the preparation of MMMs, the selection of both polymer and filler is of the highest importance, even when very high loadings can be obtained when using MOFs as fillers. Indeed, in the above mentioned high flux polymer containing MMMs, the use of PDMS, a hardly selective polymer, did not yield membranes above the Robeson upper bound. For an effective selective

transport, in line with the observations on zeolite-MMMs, it becomes essential to select a proper MOF, but also a good polymer: best when it is located closest to or on the Robeson upper bound.

Nair and co-workers [57] reported the outstanding performance of ZIF-90@6FDA-DAM MMMs, demonstrating that the combination of a selective, functionalized, MOF with a properly chosen high flux polymer may result in membranes outperforming the state of the art polymeric membranes. 6FDA-DAM ((6FDA: 2,2-bis (3,4-carboxyphenyl) hexafluoro- propane dianhydride, DAM: diaminomesitylene) has large amounts of unrelaxed free volume allowing elevated permeabilities; furthermore, the large fluorinated groups make the polymer quite rigid, providing good selective properties.[92] On the contrary, the same nanoporous material (ZIF-90) embedded in less permeable polyimides resulted in membranes with enhanced separation properties but far below the Robeson upper bound, exemplifying the importance of both MOF and polymer.

More recently, ZIF-8/6FDA-DAM MMMs were also explored for propylene/propane separations [73]. The authors observed good adhesion between the phases without the unfavourable “sieve-in-a-cage” morphology due to the hydrophobic nature of ZIF-8 as verified by TGA. Pure gas permeation showed significantly enhanced  $C_3H_6/C_3H_8$  separation over the pure 6FDA-DAM membrane performance. By adding 48 wt. % of ZIF-8 to the polymer matrix a  $C_3H_6$  permeability of 56.2 Barrer and a  $C_3H_6/C_3H_8$  selectivity of 31.0 were reached.

In the same context, Liu et al. [72] reported the efficient recovery of bio-alcohols by means of pervaporation using MMMs composed of ZIF-8 nanoparticles and silicon rubber polymethylphenylsiloxane (PMPS) coated on the inside surface of

alumina capillary substrates. Separation factor and permeability (dilute aqueous solutions (1.0 wt. %) of ethanol, *n*-propanol, *n*-butanol and *n*-pentanol alcohols increased simultaneously as the ZIF-8 loading in the composite membrane so did, demonstrating a bright future of MOF containing MMMs also in liquid separations.

#### **4. Conclusions and future perspectives**

MOFs offer many opportunities for the preparation of MMMs. The combination of an almost unlimited number of topologies, with flexibility and the possibility of including interacting organic sites in the framework, together with the high specificity of MOFs for adsorptive applications opens the door to almost unlimited possibilities in the rational design of MMMs. More importantly, in contrast to purely crystalline membranes (i.e. those made of zeolitic or MOF materials), reproducible synthesis does not seem to be an issue in the case of MMMs and no expensive supports are needed, pointing at a relatively easy and cheap scale up of this type of membranes. Last but not least, MOF particles surrounded by polymers will probably be much more stable than the bare MOF and the long term stability (of course to be assessed under industrial conditions) of such membranes should not pose an issue. Although there is still a long road ahead, we believe that the works published to date are an excellent basis for future developments. Having said that many new challenges and opportunities arise for both industry and the scientific community, below we discuss the most important ones.

*The selection of the appropriate MOF-polymer couple* is crucial for the success of MOF-based MMMs. This fact makes more challenging the field of research, since the collaboration between experts in different chemistry and

engineering fields is a must. The published results so far demonstrate that rubbery polymers might offer several advantages for application, since high fluxes can be achieved. On the other hand, MOFs with functional organic sites seem to outperform non-functional ones, since the interaction MOF-polymer is clearly improved. However, given the large library of MOFs and polymers, a significant development in theoretical predictions is needed, [25] making this field of research even more challenging and multidisciplinary. The latter is not trivial, since the developed models have to take into account flux through the polymeric matrix, through the microporous filler and through their interface.

Another point of attention should be the comparison of different membranes and the applicability of Robeson plots. In principle, these representations are valid for ideal separation factors (obtained from single component permeation data), measured at room temperature and with low driving forces ( $\Delta P = 1$  bar).[10] Although very useful for a fast screening of materials, when potential industrial applications are considered, it is easy to realize that the relevance of data obtained under such conditions is, at least, doubtful. At this point, much higher driving forces that would allow higher net fluxes and the use of gas mixtures should be explored. It goes without saying that the role of industry in providing targets in terms of gas composition, operating pressures/temperatures and durability of membranes is crucial.

From a more scientific point of view, it is fair to admit that the understanding of MMMs is still at its early infancy. Even though MMMs are by no means young, contrary to other research fields like catalysis, hardly any tool, if any, has been developed to *study membranes at work*. In this sense, the development of membrane

modules where different spectroscopic techniques could be applied *in situ* might yield very important information about filler loading, diffusion through the different components and possible aging of the membranes. With this information in hand, the development of new generations of MMMs along with more accurate mathematical models would become easier.

As discussed along the text, *flexibility* is one of the most thrilling properties of many MOFs. From the gas separation perspective, the most immediate consequence is that the concept of shape selectivity might need to be re-visited for most MOF structures. On one side, many MOFs have been shown to undergo very important changes in unit cell, volume and pore size upon adsorption (breathing phenomenon). The consequences of such breathing on MMMs need to be thoroughly investigated. We observed a positive effect of flexibility on high-pressure applications that might help overcoming long standing polymer problems such as plasticization. However, we also observed a certain expansion of the MOF filler upon membrane preparation, whether those changes might affect membrane performance need to be unravelled. On the other hand, ZIF materials have been the most widely used fillers in the works published so far in the literature. Although usually ZIFs present pore dimensions that would be ideal for the separation of small molecules, some of us have recently shown that ZIFs like ZIF-7 ( $\text{Zn}(\text{benzimidazole})_2$ ) are able to adsorb olefins and paraffins larger than the crystallographic pore size of the structure (0.3 nm). We attributed the reversed shape selectivity to a “*gate-opening*” effect due to the rotation of the benzimidazole linkers in which specific threshold pressures control the rotation of the linker and therefore the uptake and release of individual molecules.[79, 93] Aguado et al. later discussed

a similar gate opening behavior of ZIF-7 upon CO<sub>2</sub> adsorption.[94] These results combined with recent work of Luebbers et al.,[95] who demonstrated the high flexibility of ZIF-8 towards adsorption of bulky hydrocarbons, and with recent patents dealing with the application of ZIF-7 in the selective separation of CO<sub>2</sub> and the separation of CH<sub>4</sub> from different hydrocarbons,[96-99] infer that ZIFs may be much more flexible than initially anticipated.[100] Whether this flexibility is still present and whether it might affect MMM performance is not clear either.

From the membrane design perspective, more specifically from the filler engineering, much more can be done at several length scales. Further improvements in polymer-MOF matching can be achieved at both the molecular and the particle level. The first examples of a better chemical interaction via hydrogen bonding have been given already, and the use of organic functional sites at the MOF linkers seems to be a very powerful approach. In this sense, the sequential surface functionalization method developed by Kitagawa and co-workers for gas adsorption [101] might be a good approach to enhance affinity while maximizing diffusion inside the framework. In addition, there is still a lot of room for improvement from the particle engineering side of MOF-MMMs. For instance, highly loaded membranes can be obtained if no agglomeration of nanoparticles takes place by proper stabilization. On the other hand, the use of more engineered fillers, like for instance hollow spheres[102] might result in enhanced transport and very good MOF dispersion in the polymeric matrix, as shown in the case of zeolite containing MMMs. [14, 15] Another approach towards highly selective MOF containing MMMs might be the use of gas permeating selective flakes, as shown in the case of layered zeolites. [103-106] By using size

selective flakes, a much longer diffusion path for the non-permeating species might result in an enhanced selectivity for the filler permeating species.

In order to realize these and other particle engineering ideas, much more needs to be known about MOF crystallization. Surprisingly, little attention has been devoted in literature to understanding the crystallization mechanism of MOFs and to their engineering at the particle level. Only a small number of mono technique *ex-situ* crystallization studies on the synthesis of different prototypical MOFs have been reported up to date; most notably studies using X-ray absorption,[107] dynamic light scattering,[108] atomic force spectroscopy[109] and X-ray diffraction.[110] Only a few *in-situ single* technique diffraction studies under hydrothermal synthesis conditions have been published [111-113] until the first *in situ* multi-technique works on more complex MOF systems were reported. [114, 115] These studies might open the door to a rational design of synthesis conditions targeting specific textural properties.

As suggested in [63], the binary filler combinations in PSF-based MMMs explored by Zornoza et al. pointed not only at MOF-zeolite but also at MOF-MOF, zeolite-zeolite and other filler combinations, including ordered mesoporous materials, that could be examined in the search for improvements in gas separation performance. It was suggested that these combinations may lead to synergetic effects producing MMMs beyond the state-of-the-art composites. Some expected results would be: i) the improvement in the filler dispersion homogeneity (due to the combination of particles with different surface chemistry, chemical composition and degree of hydrophobicity); ii) the reduction of the optimum loading to achieve best permeability-selectivity results (and hence the possibility of keeping constant the

mechanical properties of parent polymers); iii) the possibility of producing multifunctional MMMs to afford, for instance, the separation of multicomponent mixtures (the common situation in gas separation membrane publications is the study of binary mixtures); iv) finally, this approach of filler combination allows the separate optimization of size, chemistry, porosity and external porosity of fillers in search for the above mentioned synergy, not only for gas separation applications but also for liquid separation membranes and membrane reactors.

From the membrane preparation perspective, the method used currently (dissolution of the polymer followed by solvent evaporation) could be further improved if the pioneering works by Kitagawa and co-workers on polymerization inside MOF nanochannels are considered.[116-124] Once the basis of the process has been gathered, it is easy to envisage that MOF nanoparticles can be linked to each other to form continuous MOF layers, for instance, by direct polymerization of monomers at the external surface of the MOF nanoparticles. Last but not least, although self-supported flat and coated membranes are ideal for laboratory research, one has to realize that these are not going to be the shapes of choice for an eventual industrial application of MOF based MMMs. In this regard, highly intensified hollow fibre and spiral wound geometries[9] hold many promises and more efforts should be devoted to studying how to spin MOF-polymer blends in this shape. This is again a non-trivial task, since stabilization of the blend under spinning conditions will be critical.

Summarizing, the proofs of principle for the preparation of MOF based MMMs have been demonstrated and the resulting composites have been shown to

hold many promises. We are sure that in the next decade we will witness a rapid development of these membranes with examples of industrial applications.

### **Acknowledgements**

Financial support (MAT2010-15870, CIT-420000-2009-32) and FPU Program fellowships (B. Zornoza) from the Spanish Science and Innovation Ministry are gratefully acknowledged. J.G. gratefully acknowledges the Dutch National Science foundation (NWO-VENI) for financial support.

## **References**

- [1] J.A. Moulijn, M. Makkee and A. van Diepen in Chemical Process Technology. John Wiley & Sons, Chichester, England, (2001).
- [2] J.-C. Charpentier, Chemical Engineering Journal, 134 (2007) 84.
- [3] W.J. Koros, AIChE Journal, 50 (2004) 2326.
- [4] J. Coronas and J. Santamaria, Separation and Purification Methods, 28 (1999) 127.
- [5] J. Caro and M. Noack, Microporous and Mesoporous Materials, 115 (2008) 215.
- [6] J. Gascon and F. Kapteijn, Angewandte Chemie International Edition, 49 (2010) 1530.
- [7] M.A. Aroon, A.F. Ismail, T. Matsuura and M.M. Montazer-Rahmati, Sep. Purif. Technol., 75 (2010) 229.
- [8] J. Coronas, Chemical Engineering Journal, 156 (2010) 236.
- [9] J. Caro, Current Opinion in Chemical Engineering, 1 (2011) 77.
- [10] L.M. Robeson, Journal of Membrane Science, 62 (1991) 165.
- [11] C.M. Zimmerman, A. Singh and W.J. Koros, J. Membr. Sci., 137 (1997) 145.
- [12] I.F.J. Vankelecom, E. Merckx, M. Luts and J.B. Uytterhoeven, The Journal of Physical Chemistry, 99 (1995) 13187.
- [13] B. Zornoza, P. Gorgojo, C. Casado, C. Téllez and J. Coronas, Desalination and Water Treatment, 27 (2011) 42.
- [14] B. Zornoza, S. Irusta, C. Tellez and J. Coronas, Langmuir, 25 (2009) 5903.
- [15] B. Zornoza, O. Esekile, W.J. Koros, C. Tellez and J. Coronas, Sep. Purif. Technol., 77 (2011) 137.
- [16] T.-S. Chung, L.Y. Jiang, Y. Li and S. Kulprathipanja, Prog. Polym. Sci., 32 (2007) 483.
- [17] R. Mahajan, R. Burns, M. Schaeffer and W.J. Koros, J. Appl. Polym. Sci., 86 (2002) 881.
- [18] T.-H. Bae, J. Liu, J.S. Lee, W.J. Koros, C.W. Jones and S. Nair, J. Am. Chem. Soc., 131 (2009) 14662.
- [19] O.G. Nik, X.Y. Chen and S. Kaliaguine, J. Membr. Sci., 379 (2011) 468.
- [20] P.S. Goh, A.F. Ismail, S.M. Sanip, B.C. Ng and M. Aziz, Separation and Purification Technology, 81 (2011) 243.
- [21] J. Gascon, U. Aktay, M.D. Hernandez-Alonso, G.P.M. van Klink and F. Kapteijn, Journal of Catalysis, 261 (2009) 75.
- [22] Z.Q. Wang and S.M. Cohen, Chemical Society Reviews, 38 (2009) 1315.
- [23] A.J. Fletcher, K.M. Thomas and M.J. Rosseinsky, Journal of Solid State Chemistry, 178 (2005) 2491.
- [24] G. Ferey and C. Serre, Chemical Society Reviews, 38 (2009) 1380.
- [25] H. Yehia, T.J. Pisklak, J.P. Ferraris, K.J. Balkus and I.H. Musselman, Polymer Preprints, 45 (2004) 35.
- [26] W.J. Koros, Y.H. Ma and T. Shimidzu, IUPAC Recommendations 1996 - Macromolecular Division Commission on Functional Polymers. IUPAC. Pure & Appl. Chem., Vol. 68, (1996) No. 7, pp. 1479-1489
- [27] G.S. Sur, H.L. Sun, S.G. Lyu and J.E. Mark, Polymer, 42 (2001) 9783.

- [28] Y. Zhang, K.J. Balkus Jr, I.H. Musselman and J.P. Ferraris, *Journal of Membrane Science*, 325 (2008) 28.
- [29] Y.F. Zhang, I.H. Musseman, J.P. Ferraris and K.J. Balkus, *Journal of Membrane Science*, 313 (2008) 170.
- [30] T. Yang, Y. Xiao and T.-S. Chung, *Energy & Environmental Science*, 4 (2011) 4171.
- [31] A. Car, C. Stropnik and K.V. Peinemann, *Desalination*, 200 (2006) 424.
- [32] M.J.C. Ordoñez, K.J. Balkus, J.P. Ferraris and I.H. Musselman, *Journal of Membrane Science*, 361 (2010) 28.
- [33] M. Moaddeb and W.J. Koros, *Journal of Membrane Science*, 125 (1997) 143.
- [34] R.M. Barrer and J.H. Petropoulos, *British Journal of Applied Physics*, 12 (1961) 691.
- [35] E.L. Cussler, *Journal of Membrane Science*, 52 (1990) 275.
- [36] R.H.B. Bouma, A. Checchetti, G. Chidichimo and E. Drioli, *J. Membr. Sci.*, 128 (1997) 141.
- [37] D.Q. Vu, W.J. Koros and S.J. Miller, *Journal of Membrane Science*, 211 (2003) 335.
- [38] J.A. Sheffel and M. Tsapatsis, *Journal of Membrane Science*, 295 (2007) 50.
- [39] J.A. Sheffel and M. Tsapatsis, *Journal of Membrane Science*, 326 (2009) 595.
- [40] F. Kapteijn, W. Zhu, J.A. Moulijn and T.Q. Gardner, in A. Cybulski and J.A. Moulijn (Editors), *Structured catalysts and reactors*, Second ed., CRC Taylor & Francis, Boca Raton, USA, 2006, p. 700.
- [41] R. Krishna and J.A. Wesselingh, *Chemical Engineering Science*, 52 (1997) 861.
- [42] J. van den Bergh, J. Gascon and F. Kapteijn, in J. Cejka, A. Corma and S.I. Zones (Editors), *Zeolites and Catalysis: Synthesis, Reactions and Applications*, Vol. 1, 2010, p. 361.
- [43] J.M. van de Graaf, F. Kapteijn and J.A. Moulijn, *Journal of Membrane Science*, 144 (1998) 87.
- [44] J.M. van de Graaf, F. Kapteijn and J.A. Moulijn, *AIChE Journal*, 45 (1999) 497.
- [45] R. Krishna and J.M. van Baten, *Chemical Engineering Science*, 64 (2009) 3159.
- [46] A.L. Myers and J.M. Prausnitz, *AIChE Journal*, 11 (1965) 121.
- [47] F. Kapteijn, J.A. Moulijn and R. Krishna, *Chemical Engineering Science*, 55 (2000) 2923.
- [48] R. Baur and R. Krishna, *Catalysis Today*, 105 (2005) 173.
- [49] M. Murthi and R.Q. Snurr, *Langmuir*, 20 (2004) 2489.
- [50] S. Keskin and D.S. Sholl, *Energy & Environmental Science*, 3 (2010) 343.
- [51] R. Mahajan and W.J. Koros, *Industrial & Engineering Chemistry Research*, 39 (2000) 2692.
- [52] R.T. Chern, W.J. Koros, B. Yui, H.B. Hopfenberg and V.T. Stannett, *Journal of Polymer Science: Polymer Physics Edition*, 22 (1984) 1061.
- [53] J.R. Li, R.J. Kuppler and H.C. Zhou, *Chemical Society Reviews*, 38 (2009) 1477.
- [54] R. Mahajan, R. Burns, M. Schaeffer and W.J. Koros, *J. Appl. Polym. Sci.*, 86 (2002) 881.

- [55] R. Mahajan, D.Q. Vu and W.J. Koros, *Journal of the Chinese Institute of Chemical Engineers*, 33 (2002) 77.
- [56] C.M. Zimmerman, R. Mahajan and W.J. Koros, *Abstracts of Papers of the American Chemical Society*, 214 (1997) 270.
- [57] T.H. Bae, J.S. Lee, W. Qiu, W.J. Koros, C.W. Jones and S. Nair, *Angewandte Chemie - International Edition*, 49 (2010) 9863.
- [58] B. Zornoza, C. Tellez and J. Coronas, *Journal of Membrane Science*, 368 (2011) 100.
- [59] L.M. Robeson, *Journal of Membrane Science*, 320 (2008) 390.
- [60] J.G. Won, J.S. Seo, J.H. Kim, H.S. Kim, Y.S. Kang, S.J. Kim, Y.M. Kim and J.G. Jegal, *Advanced Materials*, 17 (2005) 80.
- [61] K. Díaz, L. Garrido, M. López-González, L.F.d. Castillo and E. Riande, *Macromolecules*, 43 (2010) 316.
- [62] B. Zornoza, A. Martinez-Joaristi, P. Serra-Crespo, C. Tellez, J. Coronas, J. Gascon and F. Kapteijn, *Chemical Communications*, 47 (2011) 9522.
- [63] B. Zornoza, B. Seoane, J.M. Zamaro, C. Téllez and J. Coronas, *Chemphyschem*, 12 (2011) 2781.
- [64] B. Seoane, J.M. Zamaro, C. Tellez and J. Coronas, *RSC Advances*, 1 (2011) 917.
- [65] K. Diaz, M. Lopez-Gonzalez, L.F. del Castillo and E. Riande, *Journal of Membrane Science*, 383 (2011) 206.
- [66] R. Adams, C. Carson, J. Ward, R. Tannenbaum and W. Koros, *Microporous and Mesoporous Materials*, 131 (2010) 13.
- [67] E.V. Perez, K.J. Balkus, J.P. Ferraris and I.H. Musselman, *J. Membr. Sci.*, 328 (2009) 165.
- [68] S. Basu, A. Cano-Odena and I.F.J. Vankelecom, *Journal of Membrane Science*, 362 (2010) 478.
- [69] J. Hu, H.P. Cai, H.Q. Ren, Y.M. Wei, Z.L. Xu, H.L. Liu and Y. Hu, *Industrial & Engineering Chemistry Research*, 49 (2010) 12605.
- [70] S. Basu, A. Cano-Odena and I.F.J. Vankelecom, *Separation and Purification Technology*, 81 (2011) 31.
- [71] S. Basu, M. Maes, A. Cano-Odena, L. Alaerts, D.E. De Vos and I.F.J. Vankelecom, *Journal of Membrane Science*, 344 (2009) 190.
- [72] X.L. Liu, Y.S. Li, G.Q. Zhu, Y.J. Ban, L.Y. Xu and W.S. Yang, *Angewandte Chemie - International Edition*, 50 (2011) 10636.
- [73] C. Zhang, Y. Dai, J.R. Johnson, O. Karvan and W.J. Koros, *Journal of Membrane Science*, (2011).
- [74] C. Liu, B. McCulloch, S.T. Wilson, A.I. Benin and M.E. Schott, *US 7637983*, 2009
- [75] R. Banerjee, A. Phan, B. Wang, C. Knobler, H. Furukawa, M. O'Keeffe and O.M. Yaghi, *Science*, 319 (2008) 939.
- [76] K.S. Park, Z. Ni, A.P. Cote, J.Y. Choi, R.D. Huang, F.J. Uribe-Romo, H.K. Chae, M. O'Keeffe and O.M. Yaghi, *Proceedings of the National Academy of Sciences of the United States of America*, 103 (2006) 10186.
- [77] C. Serre, S. Bourrelly, A. Vimont, N. Ramsahye, G. Maurin, P. Llewellyn, M. Daturi, Y. Filinchuk, O. Leynaud, P. Barnes and G. Férey, *Advanced Materials*, 19 (2007) 2246.

- [78] C. Serre, F. Millange, C. Thouvenot, M. Nogues, G. Marsolier, D. Louer and G. Ferey, *J. Am. Chem. Soc.*, 124 (2002) 13519.
- [79] J. van den Bergh, C. Gücüyener, E.A. Pidko, E.J.M. Hensen, J. Gascon and F. Kapteijn, *Chemistry – A European Journal*, 17 (2011) 8832.
- [80] G. Ferey, M. Latroche, C. Serre, F. Millange, T. Loiseau and A. Percheron-Guegan, *Chemical Communications*, (2003) 2976.
- [81] T. Loiseau, C. Serre, C. Huguenard, G. Fink, F. Taulelle, M. Henry, T. Bataille and G. Ferey, *Chemistry-a European Journal*, 10 (2004) 1373.
- [82] S. Bourrelly, P.L. Llewellyn, C. Serre, F. Millange, T. Loiseau and G. Ferey, *Journal of the American Chemical Society*, 127 (2005) 13519.
- [83] F. Millange, N. Guillou, R.I. Walton, J.M. Greneche, I. Margiolaki and G. Ferey, *Chem. Commun.*, (2008) 4732.
- [84] F. Millange, C. Serre, N. Guillou, G. Ferey and R.I. Walton, *Angew. Chem., Int. Ed.*, 47 (2008) 4100.
- [85] C. Volkringer, T. Loiseau, N. Guillou, G. Ferey, E. Elkaim and A. Vimont, *Dalton Transactions*, (2009) 2241.
- [86] J. Caro, M. Noack and P. Kölsch, *Adsorption*, 11 (2005) 215.
- [87] W.D. Zhu, P. Hrabanek, L. Gora, F. Kapteijn and J.A. Moulijn, *Ind. Eng. Chem. Res.*, 45 (2006) 767.
- [88] W. Zhu, F. Kapteijn and J.A. Moulijn, *Sep. Purif. Technol.*, 32 (2003) 223.
- [89] H. Voß, A. Diefenbacher, G. Schuch, H. Richter, I. Voigt, M. Noack and J. Caro, *J. Membr. Sci.*, 329 (2009) 11.
- [90] J. van den Bergh, W. Zhu, J. Gascon, J.A. Moulijn and F. Kapteijn, *J. Membr. Sci.*, 316 (2008) 35.
- [91] Y. Li, M. Pera-Titus, G. Xiong, W. Yang, E. Landrison, S. Miachon and J.A. Dalmon, *Journal of Membrane Science*, 325 (2008) 973.
- [92] K. Tanaka, M. Okano, H. Toshino, H. Kita and K.I. Okamoto, *Journal of Polymer Science Part B-Polymer Physics*, 30 (1992) 907.
- [93] C. Gücüyener, J. van den Bergh, J. Gascon and F. Kapteijn, *Journal of the American Chemical Society*, 132 (2010) 17704.
- [94] S. Aguado, G. Bergeret, M.P. Titus, V. Moizan, C. Nieto-Draghi, N. Bats and D. Farrusseng, *New J. Chem.*, (2011).
- [95] M.T. Luebbbers, T. Wu, L. Shen and R.I. Masel, *Langmuir*, 26 (2010) 15625.
- [96] H.W. Deckman, P. Kortunov, Z. Ni, C.S. Paur, S.C. Reyes, J. Zengel and J.G. Santiesteban, WO2009105255-A2, WO2009105255-A2; US2009214407-A1; WO2009105255-A3; AU2009215790-A1; EP2249947-A2; CA2716323-A1,
- [97] H.W. Deckman, P. Kortunov, Z. Ni, C.S. Paur, J. Zengel and S.C. Reyes, WO2009105270-a2, WO2009105270-A2; WO2009105270-A3; WO2009105270-A8; AU2009215805-A1; EP2259861-A2; CA2716328-A1,
- [98] H.W. Deckman, P. Kortunov, Z. Ni, C.S. Paur, J. Zengel and S.C. Reyes, WO2009105271-A2, WO2009105271-A2; WO2009105271-A3; AU2009215806-A1; EP2249946-A2; CA2716333-A1,
- [99] H.W. Deckman, P. Kortunov, Z. Ni, C.S. Paur, J. Zengel, S.C. Reyes, J.G. Santiesteban and J.G. Sentiesteben, WO2009105251-A1, WO2009105251-A1; US2009211440-A1; US2009211441-A1; US2009216059-A1; AU2009215786-A1; EP2254683-A1; CA2716322-A1,

- [100] K.S. Park, Z. Ni, A. P., J.Y. Choi, R. Huang, F.J. Uribe-Romo, H.K. Chae, M. O'Keeffe and O.M. Yaghi, *Proceedings of the National Academy of Sciences*, 103 (2006) 10186.
- [101] K. Hirai, S. Furukawa, M. Kondo, H. Uehara, O. Sakata and S. Kitagawa, *Angewandte Chemie International Edition*, (2011) *Angew. Chem. Int. Ed.* (2011), 50, 8057–8061.
- [102] R. Ameloot, F. Vermoortele, W. Vanhove, M.B.J. Roeffaers, B.F. Sels and D.E. De Vos, *Nat Chem*, 3 (2011) 382.
- [103] H.K. Jeong, W. Krych, H. Ramanan, S. Nair, E. Marand and M. Tsapatsis, *Chem. Mater.*, 16 (2004) 3838.
- [104] M. Tsapatsis, H. Jeong, S. Nair and H.K. Jeong, WO2004000546-A1; US2004062909-A1; AU2003253697-A1; US2005037209-A1; US6863983-B2; US7087288-B2
- [105] P. Gorgojo, S. Uriel, C. Téllez and J. Coronas, *Microporous Mesoporous Mater.*, 115 (2008) 85.
- [106] C. Rubio, C. Casado, S. Uriel, C. Téllez and J. Coronas, *Materials Letters*, 63 (2009) 113.
- [107] S. Surble, F. Millange, C. Serre, G. Ferey and R.I. Walton, *Chem. Commun.*, (2006) 1518.
- [108] S. Hermes, T. Witte, T. Hikov, D. Zacher, S. Bahnmueller, G. Langstein, K. Huber and R.A. Fischer, *J. Am. Chem. Soc.*, 129 (2007) 5324.
- [109] M. Shoaee, M.W. Anderson and M.P. Attfield, *Angewandte Chemie International Edition*, 47 (2008) 8525.
- [110] N.A. Khan and S.H. Jhung, *Cryst. Growth Des.*, 10 (2010) 1860.
- [111] F. Millange, M. Medina, N. Guillou, G. Ferey, K.M. Golden and R.I. Walton, *Angewandte Chemie International Edition*, 49 (2010) 763.
- [112] F. Millange, R. El Osta, M.E. Medina and R.I. Walton, *CrystEngComm*, 13 (2011) 103.
- [113] T. Ahnfeldt, J. Moellmer, V. Guillerm, R. Staudt, C. Serre and N. Stock, *Chemistry – A European Journal*, 17 (2011) 6462.
- [114] J. Juan-Alcaniz, M. Goesten, A. Martinez-Joaristi, E. Stavitski, A.V. Petukhov, J. Gascon and F. Kapteijn, *Chemical Communications*, 47 (2011) 8578.
- [115] E. Stavitski, M. Goesten, J. Juan-Alcañiz, A. Martinez-Joaristi, P. Serra-Crespo, A.V. Petukhov, J. Gascon and F. Kapteijn, *Angewandte Chemie International Edition*, 50 (2011) 9624.
- [116] T. Uemura, N. Yanai and S. Kitagawa, *Chemical Society Reviews*, 38 (2009) 1228.
- [117] N. Yanai, T. Uemura, M. Ohba, Y. Kadowaki, M. Maesato, M. Takenaka, S. Nishitsuji, H. Hasegawa and S. Kitagawa, *Angewandte Chemie - International Edition*, 47 (2008) 9883.
- [118] T. Uemura, Y. Ono and S. Kitagawa, *Chemistry Letters*, 37 (2008) 616.
- [119] T. Uemura, Y. Ono, K. Kitagawa and S. Kitagawa, *Macromolecules*, 41 (2008) 87.
- [120] T. Uemura, S. Horike, K. Kitagawa, M. Mizuno, K. Endo, S. Bracco, A. Comotti, P. Sozzani, M. Nagaoka and S. Kitagawa, *Journal of the American Chemical Society*, 130 (2008) 6781.
- [121] T. Uemura, D. Hiramatsu, Y. Kubota, M. Takata and S. Kitagawa, *Angewandte Chemie - International Edition*, 46 (2007) 4987.

- [122] T. Uemura, R. Kitaura, Y. Ohta, M. Nagaoka and S. Kitagawa, *Angewandte Chemie - International Edition*, 45 (2006) 4112.
- [123] T. Uemura, S. Horike and S. Kitagawa, *Chemistry - An Asian Journal*, 1 (2006) 36.
- [124] T. Uemura, K. Kitagawa, S. Horike, T. Kawamura, S. Kitagawa, M. Mizuno and K. Endo, *Chemical Communications*, (2005) 5968.
- [125] L.M. Robeson, *Current Opinion in Solid State & Materials Science*, 4 (1999) 549.

**Table 1.-** Overview of the MOF-containing MMMs for gas separation chronologically reported.

MMMs		wt. % loading (best MMM performance) <sup>a</sup>	Major applications	Example (best MMM performance) <sup>b,*</sup>		Graph code <sup>c</sup>	Type of analysis	Operation condition rates (optimal value) <sup>d</sup>		Published year and reference	
MOF	Polymer			P CO <sub>2</sub> (Barrer)	CO <sub>2</sub> /CH <sub>4</sub> Selectivity			T (°C)	ΔP (bar)		
Cu(II) BPDC-TED (biphenyl dicarboxylate- triethylenediamine)	PAET	10-30 (30)	O <sub>2</sub> /N <sub>2</sub>		1.4-0.7	18.0-3.2	[A]	Single gas Gas mixture (10:90 mol %)	25	2	2004 [25]
[Cu <sub>2</sub> (PF <sub>6</sub> )(NO <sub>3</sub> )(4,4'- bpy) <sub>4</sub> ](PF <sub>6</sub> ) <sub>2</sub> (H <sub>2</sub> O) <sub>2</sub>	PSF	2.5-5 (5)	H <sub>2</sub> /CH <sub>4</sub> N <sub>2</sub> /CH <sub>4</sub>	He/CH <sub>4</sub> O <sub>2</sub> /CH <sub>4</sub>	-	-	-	Single gas	35	1	2005 [60]
HKUST-1 (Cu <sub>3</sub> (BTC) <sub>2</sub> : copper(II)-bencene- 1,3,5-tricarboxylate)	PDMS	10-40 (30)	H <sub>2</sub> /N <sub>2</sub> CO <sub>2</sub> /N <sub>2</sub>	H <sub>2</sub> /CH <sub>4</sub> O <sub>2</sub> /N <sub>2</sub>	2500- (2900)*	3.1-(3,6)*	[B1]				
	PSF	5-10 (5)	H <sub>2</sub> /N <sub>2</sub> CO <sub>2</sub> /N <sub>2</sub>	H <sub>2</sub> /CH <sub>4</sub>	6.5-(7.5)*	18.0-(21.5)*	[B2]	-	-	-	2006 [31]
Mn(HCOO) <sub>2</sub> (magnese(II)-formate)	PSF	5-10 (10)	H <sub>2</sub> /N <sub>2</sub> CO <sub>2</sub> /N <sub>2</sub>	H <sub>2</sub> /CH <sub>4</sub>	6.5-(7.0)*	18.0-(9.5)*	[B3]				
Cu-BPY-HFS (Cu-4,4' bipyridine- hexafluorosilicate)	Matrimid®	10-40 (20)	H <sub>2</sub> /N <sub>2</sub> H <sub>2</sub> /CO <sub>2</sub> H <sub>2</sub> /CH <sub>4</sub>	O <sub>2</sub> /N <sub>2</sub> CH <sub>4</sub> /N <sub>2</sub>	7.3-(9.9)	34.7-(27.6)	[C]	Single gas	35	2.7	2008 [29]
		20	H <sub>2</sub> /CO <sub>2</sub>	CH <sub>4</sub> /N <sub>2</sub>	-	36.3-(22.5)-		Gas mixture (50:50 and 10:90 mol %)			
IRMOF-1	Ultem	10-20 (10)	H <sub>2</sub> /CH <sub>4</sub>		1.95-(2.97)	30.3-(26.3)	[D1]				
	Matrimid®	20	H <sub>2</sub> /CH <sub>4</sub>		10.0-(38.8)	28.2-(29.2)	[D2]	Single gas	50	7	2009 [74]
HKUST-1	Matrimid®	30	H <sub>2</sub> /CH <sub>4</sub>		10.0-(22.1)	28.2-(29.8)	[D3]				
MOF-5	Matrimid®	10-30	H <sub>2</sub> /CH <sub>4</sub>	O <sub>2</sub> /N <sub>2</sub>	9.0-(20.2)	41.7-(44.7)	[E]	Single gas	35	2	2009

		(30)	CH <sub>4</sub> /N <sub>2</sub>									[67]
		30	CH <sub>4</sub> /N <sub>2</sub>	H <sub>2</sub> /CO <sub>2</sub>	-	38.0-(29.0)	-	Gas mixture (50:50 and 10:90 mol %)				
HKUST-1 ZIF-8 MIL-53(Al) MIL-47(V)	PDMS/ Matrimid®	5-20 (20)	Rose Bengal/isopropanol		-	-	-	(SRNF)	RT	1		2009 [71]
CuTPA (copper terephthalate)	PVAc	15	He/CH <sub>4</sub> CO <sub>2</sub> /N <sub>2</sub>	O <sub>2</sub> /N <sub>2</sub> N <sub>2</sub> /CH <sub>4</sub>	2.4-(3.3)	34.9-(40.4)	[F]	Single gas	35	4.5 (0.1 for CO <sub>2</sub> )		2010 [66]
ZIF-8	PSF	10-30 (30)	CO <sub>2</sub> transport		6-(25)		-	-	30	1, 2, 3, 5, 7,10 (10)		2010 [61]
ZIF-8	Matrimid®	20-60 (50)	O <sub>2</sub> /N <sub>2</sub> H <sub>2</sub> /O <sub>2</sub> H <sub>2</sub> /N <sub>2</sub> H <sub>2</sub> /CO <sub>2</sub>	H <sub>2</sub> /CH <sub>4</sub> CH <sub>4</sub> /N <sub>2</sub> CO <sub>2</sub> /C <sub>3</sub> H <sub>8</sub> H <sub>2</sub> /C <sub>3</sub> H <sub>8</sub>	9.5-(13)*	43.6-(124.9)	[G]	Single gas	35	2.7		2010 [32]
					-	42.1-(89.2)	-	Gas mixture (10:90 mol %)				
HKUST-1	Matrimid®	10-30 (30)	CO <sub>2</sub> /N <sub>2</sub>		10-(17.5)*	18-(24)*	[H]	Gas mixture (10:90, 35/65, 72/25 mol %)	35	10		2010 [68]
HKUST-1	Polyimide	3-6 (3)	H <sub>2</sub> /CH <sub>4</sub> CO <sub>2</sub> /N <sub>2</sub>	H <sub>2</sub> /N <sub>2</sub> , H <sub>2</sub> /O <sub>2</sub> H <sub>2</sub> /CO <sub>2</sub>	87.6-64.9 (GPU)	12-(7)*	-	Single gas	25	10		2010 [69]
ZIF-90	Ultem		CO <sub>2</sub> /N <sub>2</sub>		1.4-(2.9)	38-(39)*	[I1]		35	4.5		2010 [57]
	Matrimid®	15			7.5-(10.5)*	34-(35)*	[I2]	Gas mixture (50:50 mol %)	25	2		
	6FDA-DAM				390-(720)	24-(37)	[I3]		25			
ZIF-20	PSF	8	O <sub>2</sub> /N <sub>2</sub>		-	-	-	Gas mixture (50:50 mol %)	35	2		2011 [64]

NH <sub>2</sub> -MIL-53	PSF	16, 25, 40 (25)			3.3-(2.4)	55-(117)	[J]	Gas mixture (50:50 mol %)	-10, 35, 60, 90 (-10)	1, 3, 5, 7, 10, 13 (10)	2011 [62]
ZIF-7	PBI	10, 25, 50 (50)	H <sub>2</sub> /CO <sub>2</sub>		0.3-(24.5)*	-	-	Single gas and gas mixture (50:50 mol %)	35, 60, 80, 120, 150, 180 (180)	7	2011 [30]
ZIF-8 ZIF-8+Silicalite-1 HKUST-1 HKUST-1+Silicalite-1	PSF	16, 8+8 (16) 16, 8+8 (8+8)	H <sub>2</sub> /CH <sub>4</sub> O <sub>2</sub> /N <sub>2</sub>	CO <sub>2</sub> /N <sub>2</sub>	4.6-(12.1) 4.6-(4.9)	24.3-(19.8) 24.3-(22.4)	[K1] [K2]	Gas mixture (50:50 mol %)	35	2	2011 [63]
HKUST-1 ZIF-8 MIL-53	Matrimid®	10, 20, 30 (30)	CO <sub>2</sub> /N <sub>2</sub>		0.2-(0.7)* (GPU)	29-(33)*	-	Gas mixture (35:65 mol %)	35	5	2011 [70]
ZIF-8	PPEES	10, 20, 30 (30)	H <sub>2</sub> /N <sub>2</sub> O <sub>2</sub> /N <sub>2</sub>	C <sub>2</sub> H <sub>4</sub> /C <sub>2</sub> H <sub>6</sub>	5-(50)	22.9-(20.8)	[L]	Single gas	10, 20, 30, 40 (20)	1	2011 [65]
ZIF-8	PMPS	5-20 (15)	C <sub>2</sub> -C <sub>5</sub> alcohols/H <sub>2</sub> O		-	-	-	(PV)	80	(1.0-3.0 wt% solutions)	2011 [72]
ZIF-8	6FDA-DAM	16.4, 28,7, 48,0 (48)	C <sub>3</sub> H <sub>6</sub> /C <sub>3</sub> H <sub>8</sub>		-	-	-	Single gas and gas mixture (50:50 mol %)	35	1.4-5,5 (2)	2011 [73]

<sup>a</sup> Maximum MOF loading in terms of MMM permselectivity performance. Values are given in brackets.

<sup>b</sup> CO<sub>2</sub> permeabilities and CO<sub>2</sub>/CH<sub>4</sub> selectivities of the pure polymers and the MMMs with the optimal MOF loading. A permeance of 1 GPU corresponds to a membrane exhibiting an intrinsic permeability of 1 Barrer and having a selective layer thickness of 1 µm. Results with \* are calculated from graphs.

<sup>c</sup> Code of the different publications represented in Figure 4 and 5.

<sup>d</sup> Optimum operation conditions that maximized gas separation performance of the MMMs. Values are given in brackets.

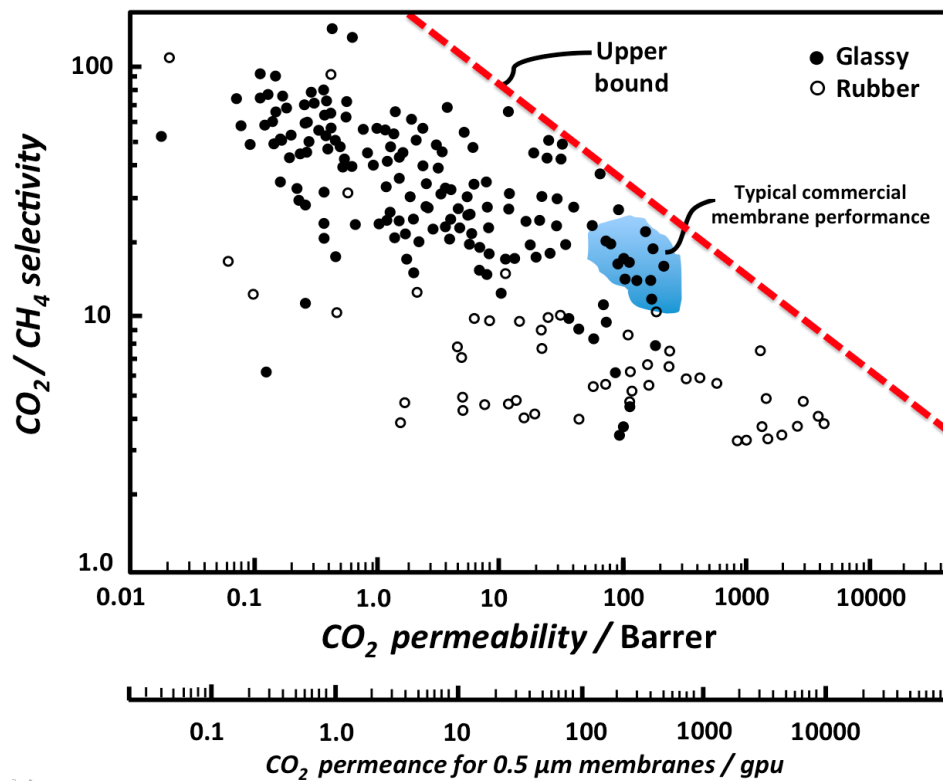


**Figure 1.-** Robeson plot for the separation of  $\text{CO}_2$  from  $\text{CH}_4$ . [125] This represents the selectivity obtained from the ratio of pure-gas permeabilities plotted against carbon dioxide permeability for different polymeric membranes. A permeance of 1 GPU corresponds to a membrane exhibiting an intrinsic permeability of 1 Barrer and having a selective layer thickness of  $1 \mu\text{m}$ .

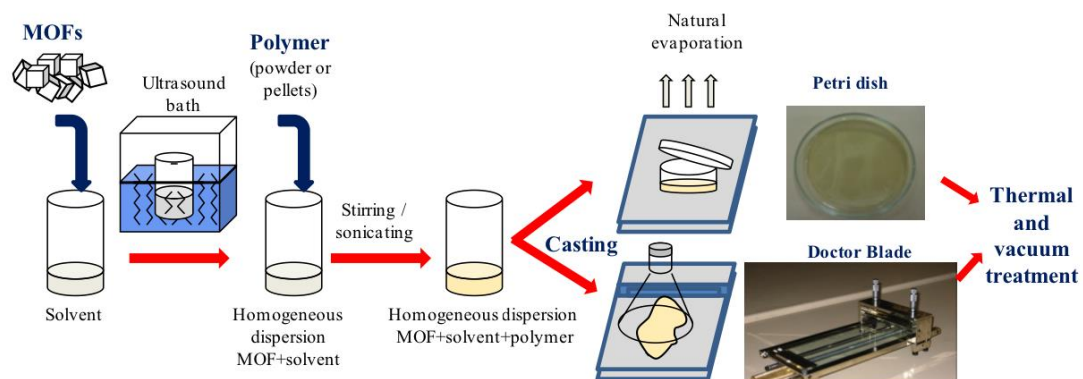


**Figure 2.-** General scheme for the fabrication of MOF-MMMs.

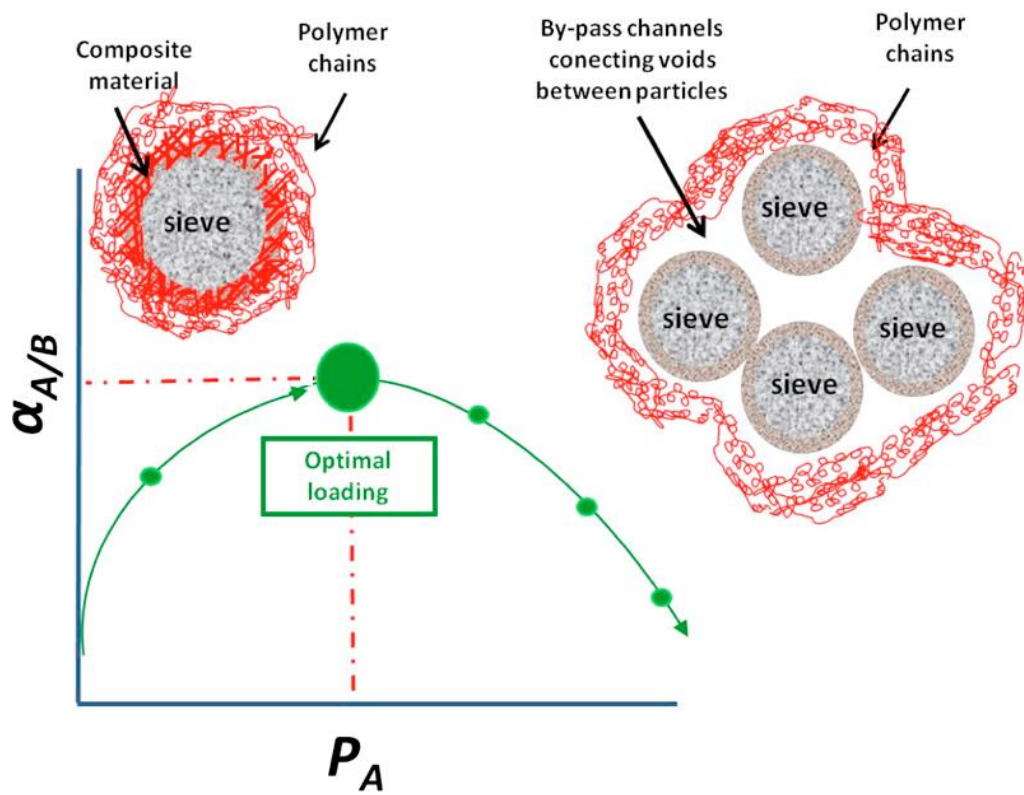


**Figure 3.-** Separation factor versus permeability of a MMM at increasing filler loading.

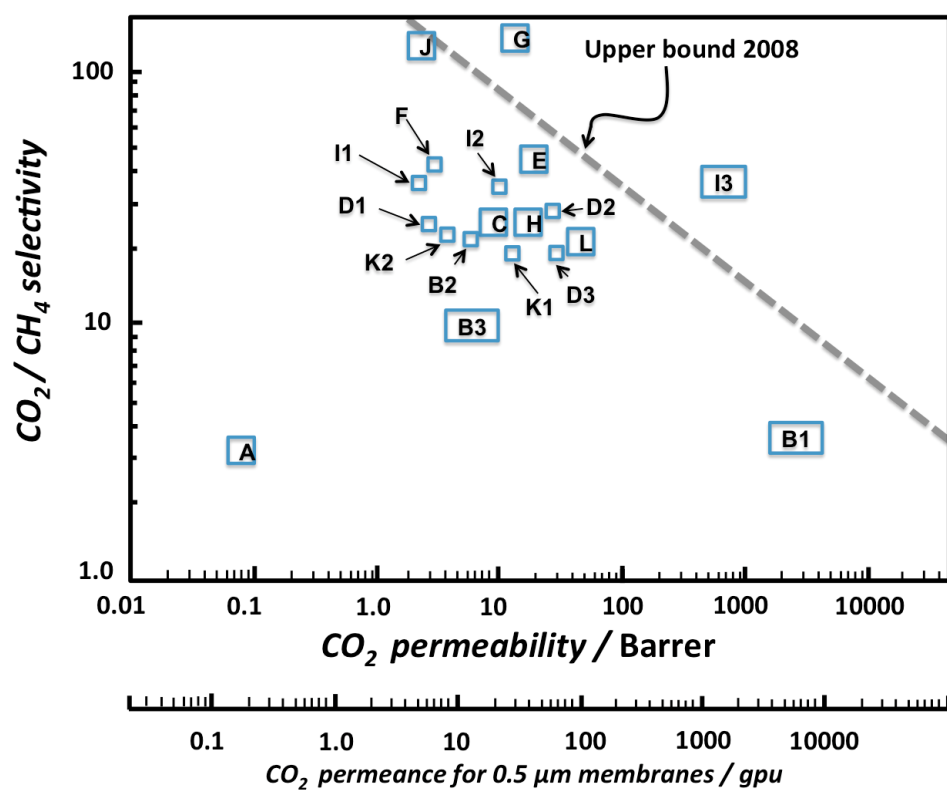


**Figure 4.-** Robeson plot containing the MOF-MMMs reported in the literature, codes for the different membranes can be found in Table1.

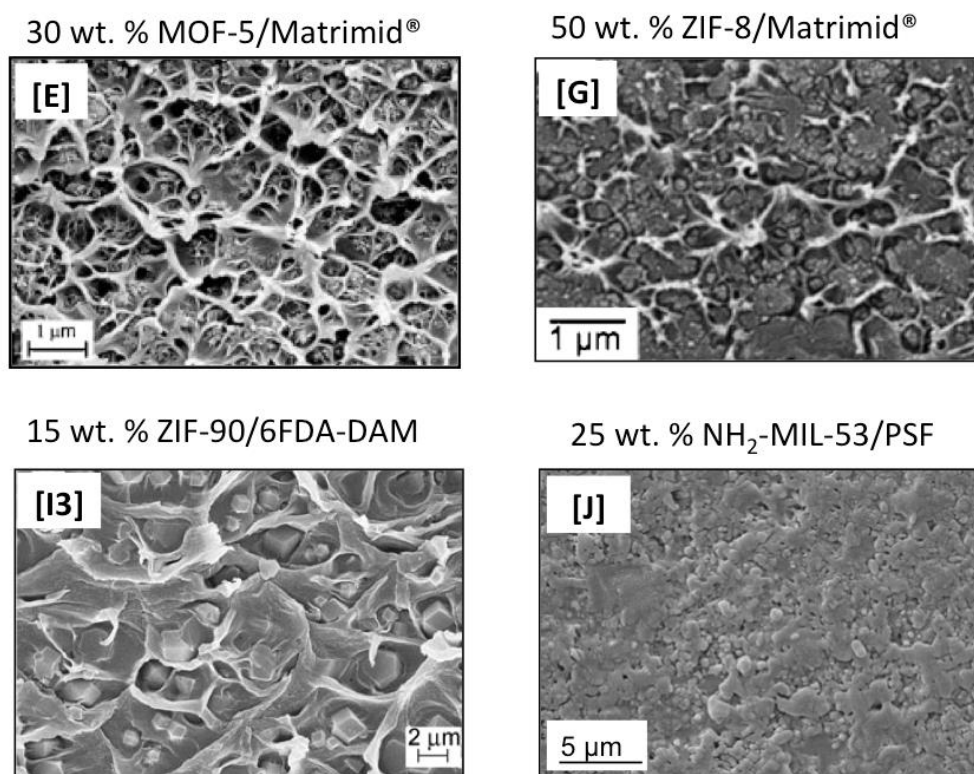


**Figure 5.-** SEM micrographs of the best MOF-MMMs reported in the literature. [32, 57, 62, 67] Codes can be found in Table 1.

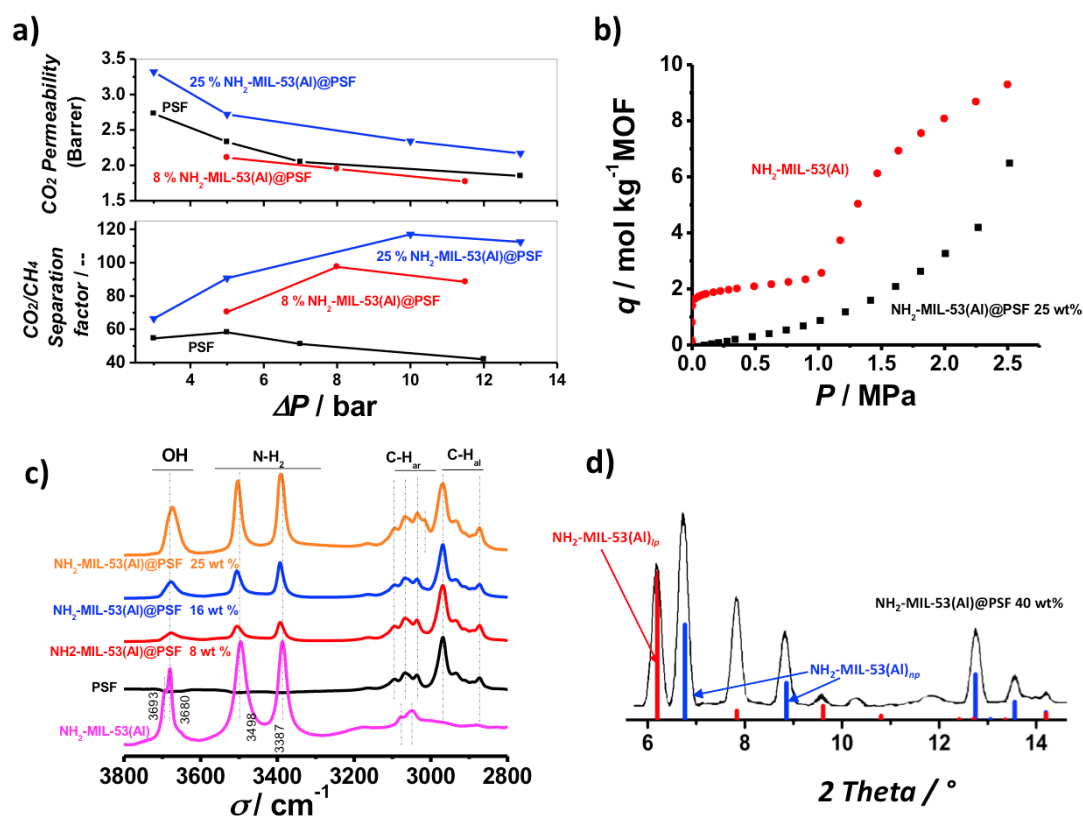


**Figure 6.-** a) Separation performance of different  $\text{NH}_2\text{-MIL-53@PSF}$  mixed matrix membranes compared to that of the parent polymer (PSF) for a mixture  $\text{CO}_2:\text{CH}_4=1:1$  as a function of the transmembrane pressure difference at 263 K ( $p_{\text{perm}} = 1$  bar) b)  $\text{CO}_2$  uptake contribution of the MOF filler at 308 K in a  $\text{NH}_2\text{-MIL-53(Al)@PSF}$  25 wt.% and the adsorption isotherm of pure  $\text{NH}_2\text{-MIL-53(Al)}$  c) Infrared spectra of pure  $\text{NH}_2\text{-MIL-53}$ , PSF and MMMs at different MOF loadings d) XRD pattern of a  $\text{NH}_2\text{-MIL-53@PSF}$  composite (wavelength = 1.12 Å). [62]